

## Supporting Information

# Aza-BODIPY fluorescent marker for CRHR1: computer design and synthesis, signaling effects, and binding constant estimation in cells

*Alan M. Szalai, Natalia G. Armando, Federico M. Barabas, Fernando D. Stefani, Luciana Giordano, Sara E. Bari, Claudio N. Cavasotto, Susana Silberstein\*, and Pedro F. Aramendia\**

### Table of Contents

#### SI Experimental Section

- 1- Computational chemistry
- 2- Synthesis and characterization
- 3- Cell lines culture and plasmids, conditions for measurements in cells
- 4- Super-resolution fluorescence microscopy. STORM imaging

#### SI Results

- 1- Computational chemistry
- 2- On the synthetic strategy of ABP-09
- 3- Solvatochromism of ABP-09
- 4- STORM performance of ABP-09 in cells
- 5- Experiments in cells and estimation of the CRHR1-ABP-09 binding constant

#### References

#### SI Experimental Section

**1: Computational chemistry.** During ligand preparation, partial atomic charges were taken from the MMFF force field [1-5]. Hydrogen atoms were added to the receptor structure using ICM, followed by a local energy minimization in the torsional space. Asp and Glu side chains were assigned a -1 charge, and all Arg and Lys side chains were assigned a +1 charge. Histidine tautomers were selected according to their hydrogen bonding pattern. In docking, the receptor was represented by six energy maps, namely, those corresponding to

electrostatic, hydrogen bond, hydrophobic, and van der Waals interactions (the latter was represented by three different maps).

**2: Synthesis and characterization.** Synthesis of aza-dipyrromethene (ADPM) and its  $\text{BF}_2$  chelated compound were performed under  $\text{N}_2$  atmosphere due to ADPM low stability when exposed to air.

Column chromatography was performed using silica gel (Silica Gel 60, 70-230 mesh). For preparative TLC, Silica Gel 60 aluminum sheets without fluorescent indicator were used. Compounds were characterized by NMR spectroscopy, UPLC/HRMS, and UV-visible absorption and emission spectroscopy as described below.

**Chemicals.** Solvents and reagents of the highest purity available were used as purchased or they were purified using standard methods when necessary. 2,4-Dimethylpyrrole (97%), 2,4-Dichlorobenzaldehyde (99%), diisopropylethylamine (DIPEA, 99.5%), nitromethane (>95%),  $\text{BF}_3 \cdot \text{OC}_4\text{H}_{10}$  (for synthesis) and diethylamine (99.5%) were all purchased to Sigma-Aldrich. For spectroscopic measurements and HRMS (direct inlet and UPLC) Optima LC/MS solvents from Fischer Chemical and Milli-Q water were used.

**NMR spectroscopy.**  $^1\text{H}$  and  $^{13}\text{C}$  NMR spectra were measured at 500 MHz and 126 MHz respectively, using a Bruker Avance II 500 spectrometer. Spectra analysis was carried out with MestReNova 11.0.4 software. For internal reference, residual solvent signals were used ( $\text{CHCl}_3$  in  $^1\text{H}$  spectra and  $\text{CDCl}_3$  for  $^{13}\text{C}$ ).  $\text{CDCl}_3$  was the only solvent used for NMR spectroscopy. Chemical shifts are reported as  $\delta$  values in ppm relative to TMS or residual solvent  $\text{CDCl}_3$  (7.26 ppm; 77.0 ppm).  $^1\text{H}$  NMR data are reported as follows: chemical shift in ppm, multiplicity (s = singlet, d = doublet, t = triplet, q = quartet), coupling constants in Hz, and relative integration in number of protons. For  $^{13}\text{C}$  NMR, only chemical shift values are reported.

**HRMS.** UPLC-HRMS was performed in a Waters ACQUITY UPLC I-Class system coupled to a Xevo G2-S QToF mass spectrometer (Waters Corp., Manchester, UK). Samples were prepared in water-acetonitrile 10:90 and UPLC gradients varied from water (0.5% formic acid): acetonitrile 80:20 as initial conditions up to 90% acetonitrile after 11 minutes. Flow rate in UPLC was 0.3 mL/min, column temperature 35°C and ionization conditions at HRMS detection varied for each compound.

**Spectroscopy.** Absorption spectra were recorded on a Shimadzu UV-3600 spectrophotometer, and fluorescence emission and excitation spectra (steady state) were measured on a PTI QM40 spectrofluorometer. Emission was corrected for the spectral sensitivity of the detection channel. Samples were contained in a 1 cm square quartz cuvette with a Teflon stopper. Fluorescent quantum yield was calculated using Rhodamine 6G as reference.

Emission time decay curves were recorded on an IBH-Horiba-Jovin-Ivon Time Correlated Single Photon Counting equipment. The sample was excited by a 1 MHz repetition rate LED (Horiba Jovin Ivon 457 nm LED, 1 ns FWHM pulse). Light passed through a monochromator before impinging on the sample in a 1 cm square quartz cuvette. Using excitation with vertically polarized light, emission was recorded at the magic angle by a red enhanced PMT after passing through an emission monochromator. Emission time profiles were recorded at single emission wavelength until 10000 counts were accumulated at the maximum. The counting rate was reduced to prevent photon pile up. A 0.055 ns/channel time calibration was used. Emission decay curves were fitted by deconvolution of the IRF using the software of the equipment.

**(E)-4-(2,4-Dichlorophenyl)but-3-en-2-one (1).** (Adapted from <sup>[6]</sup>) 2,4-

Dichlorobenzaldehyde (1.575 g, 9 mmol) was dissolved in a mixture of acetone (450 mL, excess) and water (360 mL). Aqueous solution of NaOH 5% (5 mL) was added dropwise to the reaction flask at 40°C during 1 h. After reactant consumption and disappearance of alcohol intermediate (observed by TLC), acetone was removed under reduced pressure and the precipitate was filtered and washed with water. The filtered solid was dried in vacuo to yield **1** as a white solid (1.509 g, 7.2 mmol, yield: 78%): <sup>1</sup>H NMR (500 MHz, CDCl<sub>3</sub>) δ 7.85 (d, J = 16.4 Hz, 1H), 7.57 (d, J = 8.5 Hz, 1H), 7.46 (d, J = 2.2 Hz, 1H), 7.28 (dd, J = 8.5, 2.2, 1H), 6.65 (d, J = 16.3 Hz, 1H), 2.41 (s, 3H). <sup>13</sup>C NMR (126 MHz, CDCl<sub>3</sub>) δ 198.01, 137.90, 136.59, 135.66, 131.29, 130.05, 129.82, 128.30, 127.70, 27.40 (Figure S1). ESI-HRMS [M-H]<sup>-</sup>: 212.9878, C<sub>10</sub>H<sub>7</sub>O<sub>3</sub>Cl<sub>2</sub> requires 212.9874 (Figure S3).

**4-(2,4-Dichlorophenyl)-5-nitro-butan-2-one (2).** (Adapted from <sup>[7]</sup>) (E)-4-(2,4-

Dichlorophenyl)but-3-en-2-one(1) (2.200 g, 10.25 mmol), nitromethane (3.133 g, 51.25 mmol) and diethylamine (3.754 g, 51.25 mmol) were dissolved in methanol (230 mL) and heated under reflux for 48 h. After reactant disappearance (observed by TLC), the solution was cooled and methanol was removed under reduced pressure. Water (100 mL) and CH<sub>2</sub>Cl<sub>2</sub> (100 mL) were added to the resulting oil, and successive extractions with CH<sub>2</sub>Cl<sub>2</sub> (2 x 100 mL) were carried out. The combined organic layers were dried with sodium sulfate and evaporated to dryness. After silica gel column chromatography purification, a white solid was obtained (2.474 g, 9.02 mmol, yield: 88%): <sup>1</sup>H NMR (500 MHz, CDCl<sub>3</sub>) δ 7.42 (d, J = 2.2 Hz, 1H), 7.23 (dd, J = 8.4, 2.2 Hz, 1H), 7.15 (d, J = 8.4 Hz, 1H), 4.74 (dd, J = 6.6, 1.8 Hz, 2H), 4.40 (dq, J = 7.8, 6.3 Hz, 1H), 3.05 (dd, J = 18.2, 7.8 Hz, 1H), 2.94 (dd, J = 18.1, 6.0 Hz, 1H), 2.17 (s, 3H). <sup>13</sup>C NMR (126 MHz, CDCl<sub>3</sub>) δ 205.09, 134.73, 134.56,

134.44, 130.35, 129.50, 127.82, 77.41, 77.31, 77.16, 76.91, 44.43, 35.49, 30.36, 0.14

(FigureS2). ESI-HRMS [M-H]<sup>-</sup>: 274.0036, C<sub>11</sub>H<sub>10</sub>NO<sub>3</sub>Cl<sub>2</sub> requires 274.0038 (Figure S4).

**BF<sub>2</sub> chelated (Z)-N-[3-(2,4-Dichlorophenyl)-5-methyl-2H-pyrrol-2-ylidene]-3,5-**

**dimethyl-1H-pyrrol-2-amine (ABP-09).** (Adapted from <sup>[8]</sup>) A mixture of 4-(2,4-

Dichlorophenyl)-5-nitro-butan-2-one (**2**) (1.500 g, 5.44 mmol), 2,4-dimethylpyrrole (0.516

g, 5.44 mmol), and ammonium acetate (14.6 g, 190 mmol) in methanol (32 mL) was heated

under reflux for 12 h, under a N<sub>2</sub> atmosphere. The solution was cooled, treated with

saturated NaHCO<sub>3</sub> (80 mL) and extracted with ethyl acetate (3 x 100 mL). The combined

organic layers were washed with water, brine, dried over sodium sulfate, and the solvent

removed under reduced pressure. The resulting oil contained at least 8 products in

comparable quantities and was partially purified by silica gel column chromatography. The

fraction containing compound **3** (verified by ESI-HRMS [M-H]<sup>+</sup>: 332.0721, C<sub>17</sub>H<sub>14</sub>N<sub>3</sub>Cl<sub>2</sub>

requires 332.0721, see FigureS5) was used for the next synthetic step. Prolonged

manipulation of **3** was avoided due to its high instability. The impure fraction (100 mg) was

treated with DIPEA (504.1 mg, 3.9 mmol, large excess), and BF<sub>3</sub>.OC<sub>4</sub>H<sub>10</sub> (780.3 mg, 5.5

mmol, large excess) in dry CH<sub>2</sub>Cl<sub>2</sub> under N<sub>2</sub> for 6 h. The reaction mixture was washed with

water (3x40 mL), brine (40 mL), dried over sodium sulfate, and the solvent removed under

reduced pressure. Purification by preparative TLC gave ABP-09 in very small quantities

(less than 0.1 mg), as a magenta solid. Solid purity and identity was verified by UPLC-

HRMS: [M-H]<sup>-</sup>: 377.0587, C<sub>17</sub>H<sub>13</sub>BN<sub>3</sub>F<sub>2</sub>Cl<sub>2</sub> requires 377.0584. Figure S6 shows the

calculated and experimental isotopic mass distribution and Figure S7 depicts the UPLC

chromatograms obtained for ABP-09.

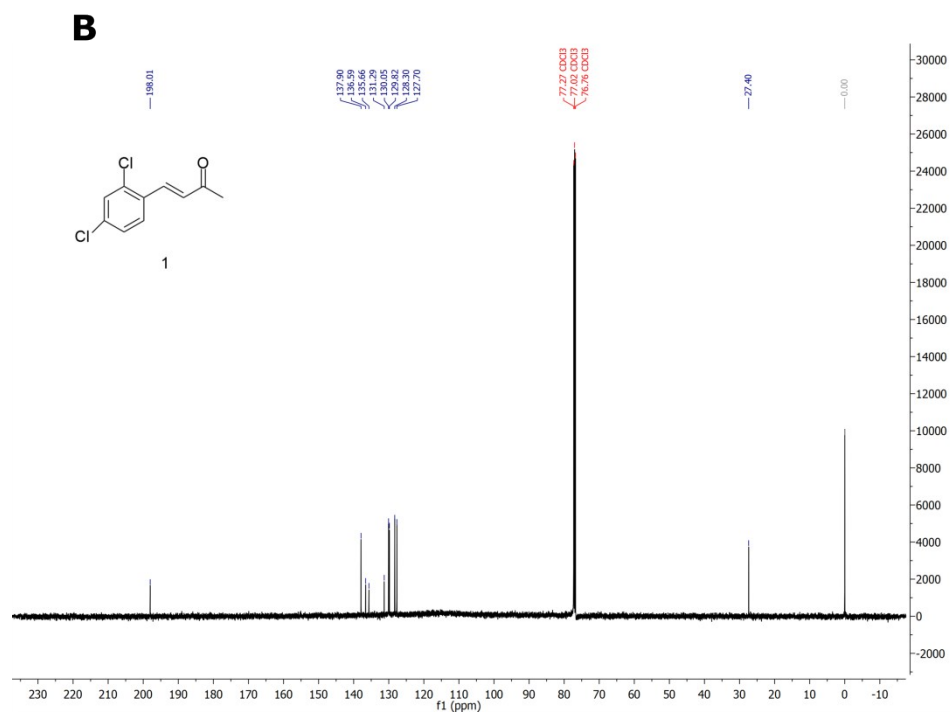
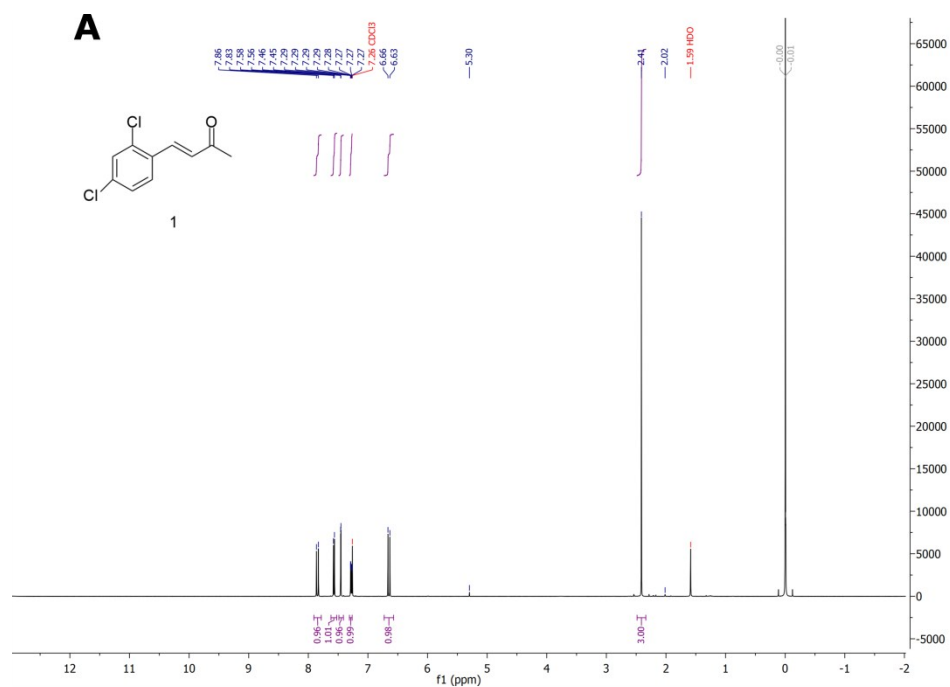


**Figure S1.** A) <sup>1</sup>H-NMR (500 MHz): Compound 1. B) <sup>13</sup>C-NMR (126 MHz): Compound 1.

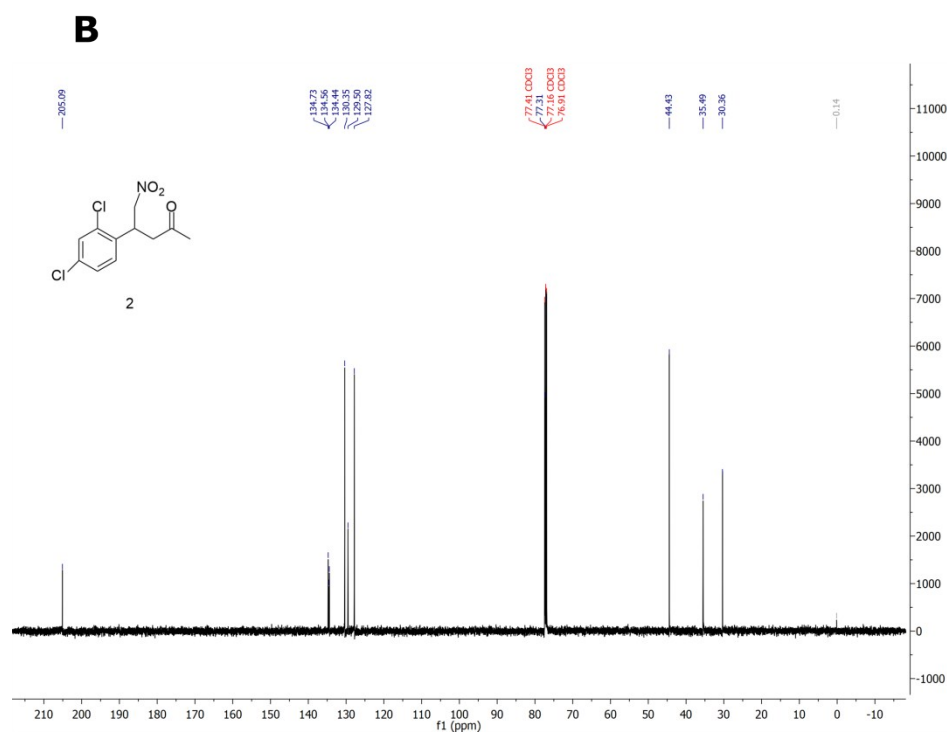
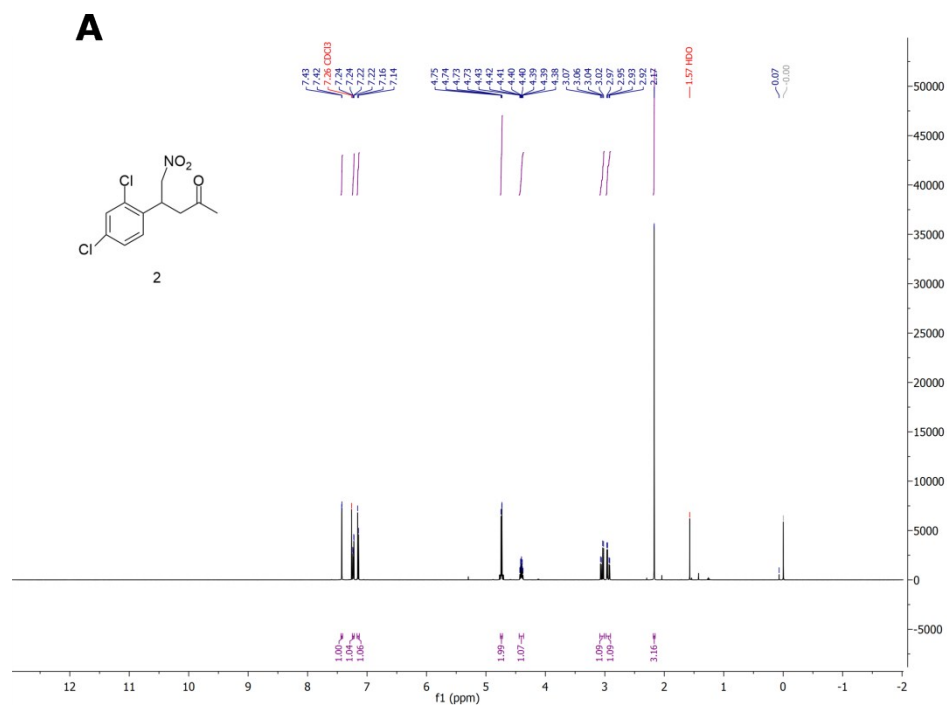
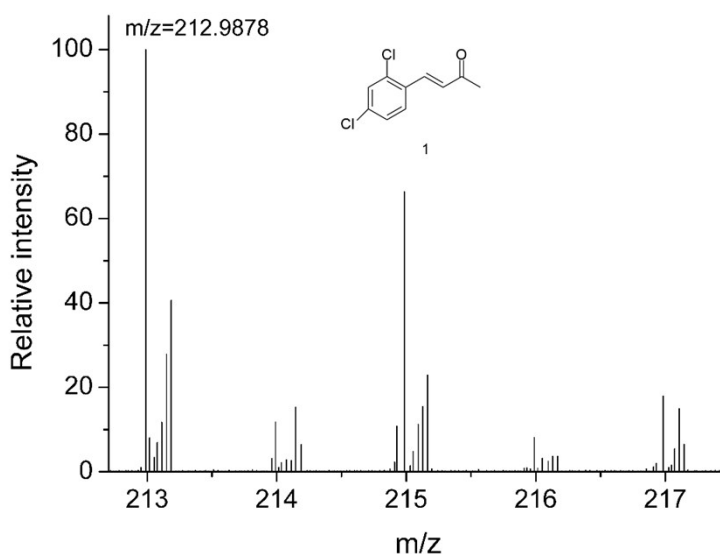
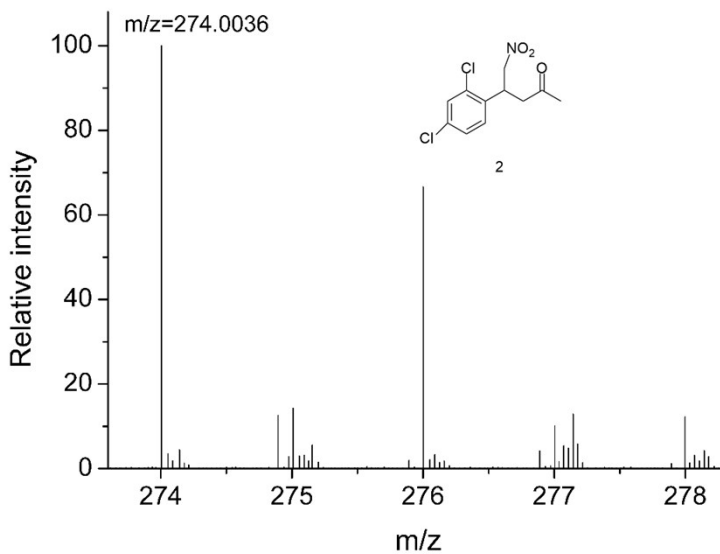


Figure S2. A)  $^1\text{H-NMR}$  (500 MHz): Compound **2**. B)  $^{13}\text{C-NMR}$  (126 MHz): Compound **2**.



**Figure S3.** HRMS (ESI<sup>-</sup>). Compound **1**. Calculated m/z (M-H<sup>-</sup>) = 212.9874. Observed: 212.9878. Ionization conditions: Capillary 2.3 kV, Sampling Cone 30 V, Source Temperature 120°C, Desolvation Temperature 300°C, Cone Gas Flow 0 L/h, Desolvation Gas Flow 400 L/h.



**Figure S4.** HRMS (ESI<sup>-</sup>). Compound **2**. Calculated m/z (M-H<sup>-</sup>) = 274.0038. Observed: 274.0036. Ionization conditions: Capillary 2.3 kV, Sampling Cone 30 V, Source Temperature 120°C, Desolvation Temperature 300°C, Cone Gas Flow 0 L/h, Desolvation Gas Flow 400 L/h.

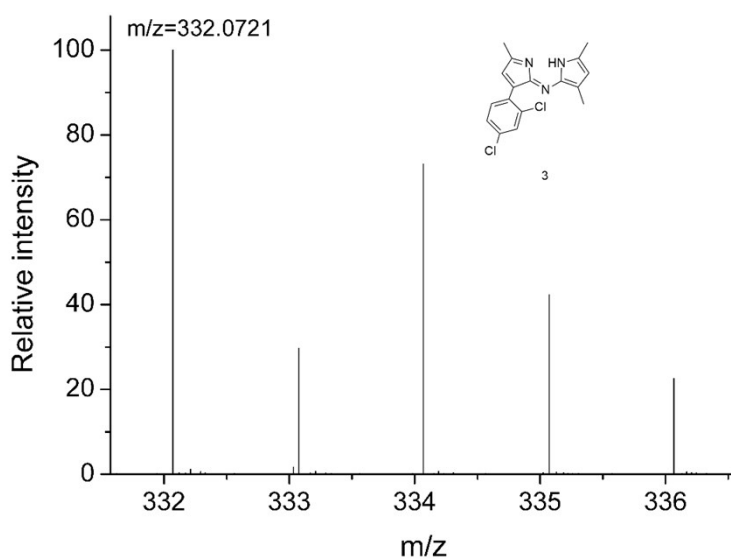


**Figure S5.** HRMS (ESI<sup>+</sup>). Compound **3**. Calculated m/z (M-H<sup>+</sup>) = 332.0721. Observed: 332.0721. Ionization conditions: Capillary 2.5 kV, Sampling Cone 30 V, Source Temperature 120°C, Desolvation Temperature 300°C, Cone Gas Flow 10 L/h, Desolvation gas flow 600 L/h

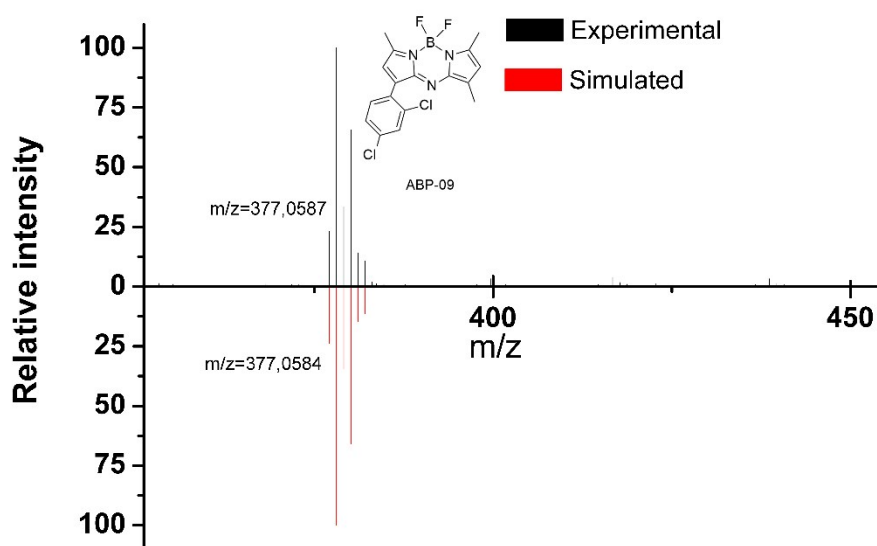


**Figure S6.** HRMS (ESI<sup>-</sup>). ABP-09. Calculated m/z (M-H<sup>-</sup>) = 377.0584. Observed: 377.0587. Ionization conditions: Capillary 2.3 kV, Sampling Cone 30 V, Source Temperature 120°C, Desolvation Temperature 300°C, Cone Gas Flow 10 L/h, Desolvation Gas Flow 600 L/h.

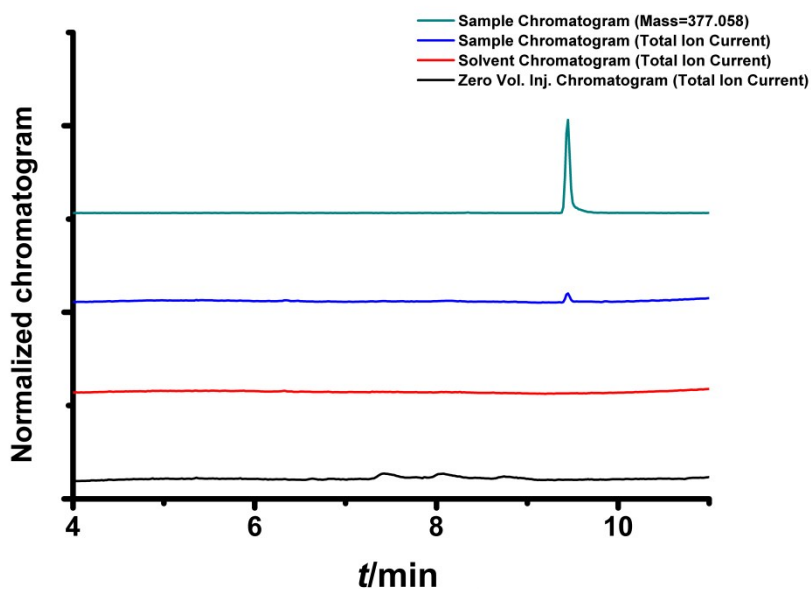


**Figure S7.** UPLC-HRMS (ESI<sup>-</sup>). ABP-09. The only peak that is detected in the sample chromatogram but not in the solvent or column chromatograms appears at 9.45 min after sample injection. This peak corresponds to ABP-09 exact mass and demonstrates the sample purity.

**3: Cell lines culture and plasmids, conditions for measurements in cells.** Mouse hippocampal neuronal cell line HT22, HT22-CRHR1 and HT22-CRHR1-Epac-S<sup>H187</sup> cells were previously described. <sup>[9, 10]</sup> Cell lines were cultured in DMEM low glucose (Invitrogen) supplemented by 5% of FBS (Natocor), 2mM L-glutamine, 50 µg/µL Geneticin (G418 selective antibiotic) when necessary, 100 U/mL penicillin and 100 µg/mL streptomycin (Invitrogen) at 37°C in a humidified atmosphere containing 5% CO<sub>2</sub>.

**Plasmids to construct the stable cell lines:** The mouse CRHR1 expression vector c-Myc-CRHR1 was provided by J. Deussing (Max Planck Institute of Psychiatry, Munich, Germany); mTurquoise2-EPAC-cp173Venus-Venus (Epac-S<sup>H187</sup>) by K. Jalink (Netherlands Cancer Institute, Amsterdam, Netherlands).

***ERK1/2 and Akt activation assays:*** HT22-CRHR1 cells were serum-starved and preincubated for 20 h in OptiMEM (Invitrogen) with DMSO (vehicle), ABP-09 or CP-376395 (3212, TOCRIS) at the concentrations indicated. After preincubation, cells were stimulated with CRH at time 0, at the indicated concentrations. After treatments with either ABP-09 or vehicle (DMSO), cells were washed with ice-cold PBS and lysed in Laemmli sample buffer. Cells lysates were sonicated and heated to 95°C for 5 min. Samples were resolved by SDS-PAGE and transferred to a 0.45 µm nitrocellulose membranes (GE Health care Life Sciences) for immunoblotting. Membranes were blocked in 0.05% Tween 20 in TBS buffer containing 5% of heat-inactivated milk (1 h at 60°C) at room temperature (RT) for 1 h and probed overnight at 4°C with primary antibodies. Secondary antibodies were incubated at RT for 1 h under shaking. The antibodies used were: anti-pERK1/2 (E-4; sc-7383) from Santa Cruz Biotechnology, Inc.; anti-total-ERK1/2 (9102); anti-pAkt (193H12) and anti-total-Akt (2920S) from Cell Signaling Technologies.

Phosphorylation of ERK1/2 and Akt, and total proteins, were detected with the Odyssey Fc Imaging system (LI-COR biosciences), using anti-mouse IRDye800CW (926-32212); IRDye680LT (926-68022) and anti-rabbit IRDye800XCW (926-32213); IRDye680LT (926-68023) (LI-COR biosciences) secondary antibodies. Phosphorylated proteins were relativized to the total protein level, and results were expressed as the percentage of maximum pERK1/2 after 5 min of stimulation or after 30 min for pAkt. Immunoreactive signals were analyzed digitally using ImageJ software (National Institutes of Health).

***Spectral FRET and imaging of cAMP:*** FRET experiments were carried out as previously described.<sup>[10]</sup> Cell imaging was performed on an inverted LSM 710 (ZEISS) microscope with an automated stage, definite focus and incubation chamber. Software ZEN black 2011

was used for data acquisition. Images were acquired with a C-Apochromat 40x NA 1.2 water immersion and temperature-corrected objective lens at 1024 x 1024 pixels, 16 bits, pixel dwell time 3.15  $\mu$ s, with open pinhole (600  $\mu$ m). The emission spectra of ABP-09 and the fluorescence proteins mTurquoise2 and Venus were determined using 405 nm laser for the excitation and lambda mode for the detection using a 32 channel QUASAR detector arranged with band-width channels of 9.7 nm. For the reference spectra and the experiments, phenol red-free DMEM medium supplemented with 20 mM Hepes was used, and imaging was performed at 37°C and 5% CO<sub>2</sub>.

Cells were illuminated with 30 mW, 405 nm diode laser at 2% power (gain: 550-650) and a 405 nm dichroic mirror; emission was collected between 413 and 723 nm every 15 s during 15 min. The saturation level was verified for each image.

For lambda mode, the linear unmixing tool of ZEN Black 2011 software was used to obtain an image for each fluorophore using the reference spectra. Quantification of the images was performed using Fiji software (ImageJ). After background subtraction FRET and donor intensities were measured for single cells for each time point. The FRET/donor ratio was calculated and normalized to resting levels before stimulation (see Movie S1).

***ABP-09 uptake followed by live imaging.*** Cell imaging was performed on a widefield inverted microscope AxioObserver Z1 (ZEISS), with an automated stage, definite focus and incubation chamber. Software ZEN black 2011 was used for data acquisition. Images were acquired with a Plan-Achromat 20x NA 0.8 air objective lens at 1040 x 1388 pixels, 14 bit, using a 60HE filter set (ZEISS) and acquiring images every 10 min in an AxioCam HRm3 camera (750 ms of exposure time). For fluorescence excitation, a 505 nm LED was used at 15% power. The total emission reported for every time point is the mean fluorescence arising from cells after subtracting the background value. For each condition,

3 fields from 3 different wells were taken into consideration (approximately 10 cells per field). Fluorescence quantification was carried out using a MATLAB routine.

***Immunofluorescence and sample preparation for STORM imaging:*** Glass coverslips of 18 mm diameter used for cell growth were sonicated at 30°C for 10 min submerged in acetone, 10 min in aqueous solution of Hellmanex III (0.05%), and 10 min in Milli-Q water. After drying at 100°C for 2 h, coverslips were treated in a Plasma Cleaner (Zepto, Diener Electronic), with air-filtered plasma (15 minutes at 20% power).

HT22 or HT22-CRHR1 cells were seeded on these treated coverslips and grown until 60% confluency.

After preincubation with ABP-09 for 20 h and treatment with CP-376395 (when necessary, i.e., in displacement assays), cells were washed with ice-cold PBS supplemented with 1M MgCl<sub>2</sub> and 1M CaCl<sub>2</sub> and fixed with 4% paraformaldehyde in PBS for 15 min. Next, cells were permeabilized with 0.01% Triton X-100 in PBS during 15 min. After washing with supplemented PBS, nonspecific binding was reduced blocking with 5% fetal bovine serum in PBS for 1 h. Primary antibody anti-c-Myc (9E10; sc-40 Santa Cruz Biotechnology, Inc.) was diluted 1:150 in blocking solution and incubated for 2 h at RT in humidified chamber. After washing with 0.05% Tween 20 in PBS, cells were incubated with Alexa Fluor 647 conjugated mouse secondary antibodies (A-21235 Thermo Fischer Scientific) diluted 1:250 in blocking solution at RT for 1 h in humidified chamber in absence of light. Controls of immunofluorescence in absence of primary antibody and in the HT22 cell line (with no expression of cMyc-CRHR1) were performed. After washing with 0.05% Tween 20 in PBS, coverslips were maintained in ice cold PBS supplemented with MgCl<sub>2</sub> and CaCl<sub>2</sub>. Minutes before imaging, the cells were mounted in a STORM Imaging Buffer (50 mM Tris pH=8 and 10 mM NaCl supplemented with 10 % w/v glucose, 100 mM

mercaptoethylamine, 1  $\mu\text{g}/\text{mL}$  glucose oxidase and 0.5  $\mu\text{g}/\text{mL}$  catalase) on microscope slides.

**4: Super-resolution fluorescence microscopy. STORM imaging.** The components of the custom-built microscope used for STORM imaging are shown in Figure S8. A 642 nm 1.5 W laser (MPB Communications 2RU-VFL-P-1500-642) was used for fluorescence excitation of Alexa Fluor 647 and a 532 nm 1.5 W laser (Laser Quantum Ventus 532) was used for fluorescence excitation of ABP-09. Both fluorophores were re-activated from their dark states with a 405 nm 50 mW laser (RGB Photonics Lambda Mini). The lasers were combined with dichroic mirrors (Semrock LM01-427 and LM01-552), magnified, and then focused to the back focal plane of the oil immersion objective Olympus PlanApo 60x NA 1.42.

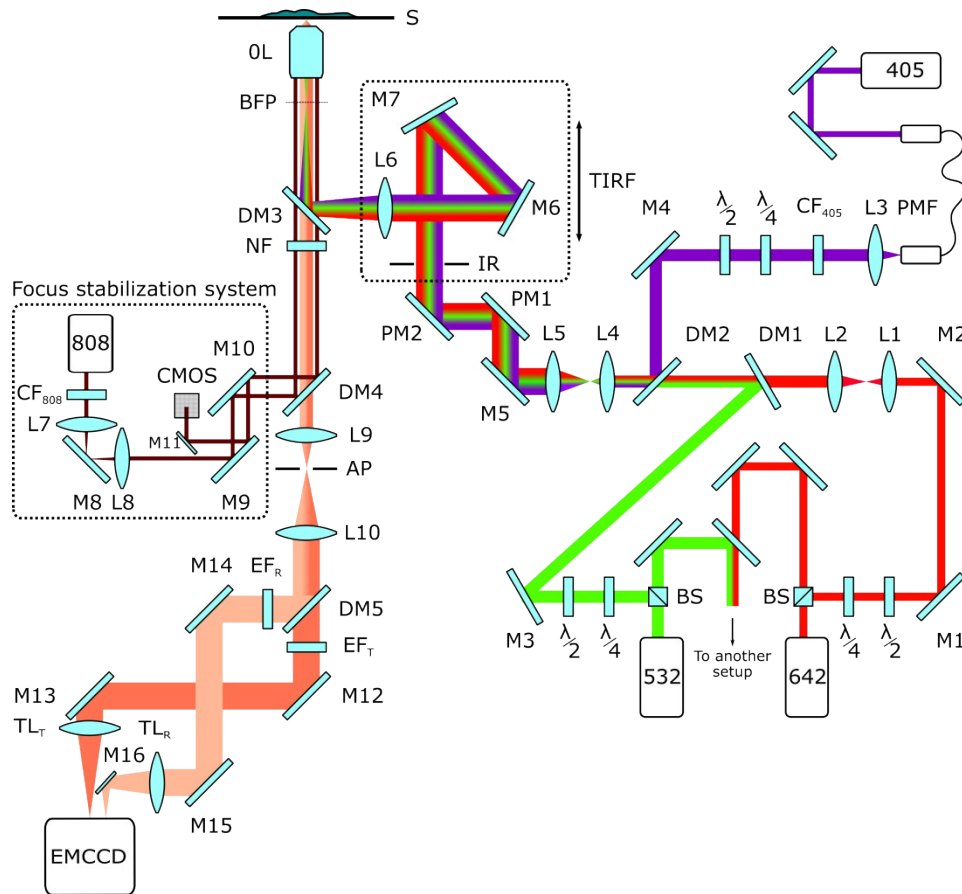


**Figure S8.** Custom-built STORM microscope. M1-15 and PM: broadband dielectric mirrors (Thorlabs BB1-E02), L1-8: achromatic doublet lenses (Thorlabs). Focal lenses (mm): 45, 75, 30, 30, 150, 200, 50, 50. L9: original tube lens of the Olympus microscope stand. L10: achromatic doublet lens (Edmund Optics) 75mm focal length. TL<sub>T</sub> and TL<sub>R</sub>: achromatic doublet lenses (Thorlabs) 150mm focal length.  $\lambda/2$  and  $\lambda/4$ : multi-order half and quarter-wave plates (Thorlabs) specific for each wavelength. CF: clean-up filters for each laser. PMF: polarization-maintaining monomode optical fiber (Thorlabs). DM1-5: dichroic mirrors: Semrock LM01-552, LM01-427, Di03-R405/488/532/635-t1, FF750-SDi02 and Chroma ZT647rdc. TIRF: motorized linear stage for total internal reflection fluorescence mode (Thorlabs). IR: iris aperture (Thorlabs). BFP: back focal plane of the objective lens. OL: objective lens (Olympus PLAPON 60x NA 1.42). NF: quad-band notch filter Semrock NF03-405/488/532/635E. CMOS: web camera. AP: rectangular aperture (Newport). EF<sub>T</sub>: emission filter Chroma ET700/75m. EF<sub>R</sub>: emission filter, Semrock 582/75 BrightLine HC. EMCCD: electron-multiplying charge coupled device camera Andor iXon3 897.

A dichroic mirror (Semrock Di03-R 405/488/532/635-t1) and a band-pass filter (Chroma ET700/75m) were used for decoupling the fluorescence emission of the sample from the laser excitation. Further blocking of the illumination lasers was performed with a multi-edge notch filter (Semrock NF03-405/488/532/635E). The emission light was expanded

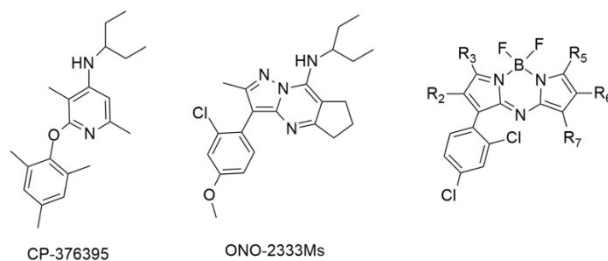
with a 2x telescope so that the pixel size of the EMCCD camera (Andor iXon3 897) would match the optimal value for single-molecule localization. Finally, fluorescent emission from different species were separated with a dichroic mirror (Chroma ZT647rdc) and imaged onto adjacent areas of the camera.

Differences in magnification, shear and image rotation between the two channels must be taken into account to obtain an accurate overlay of the final reconstructed images. This is done by imaging isolated fluorescent markers visible on both channels (Life Technologies Tetraspeck 0.1  $\mu\text{m}$ ) and then finding the affine transformation that minimizes the distance between the same markers as detected in each detection channel with a routine described previously. <sup>[11]</sup>

## SI Results

### 1: Computational chemistry

**Table S1.** aza-BODIPY basic structure and the substituent pattern for the library of compounds studied for docking with CRHR1. Also shown are antagonists CP-376395 and ONO-2333-Ms, used as reference compounds.



Structure	R <sub>2</sub>	R <sub>3</sub>	R <sub>5</sub>	R <sub>6</sub>	R <sub>7</sub>
ABP-0	H	H	Me	Me	H
ABP-01	Me	H	H	H	H
ABP-02	H	H	H	H	H
ABP-03	H	Me	H	H	H

ABP-04	Me	Me	H	H	H
ABP-05	Me	H	Me	H	H
ABP-06	Me	H	H	Me	H
ABP-07	H	Me	Me	H	H
ABP-08	H	Me	Me	H	Me
ABP-09	H	Me	Me	H	Me
ABP-10	H	H	Me	H	Me
ABP-11	Me	H	Me	H	Me

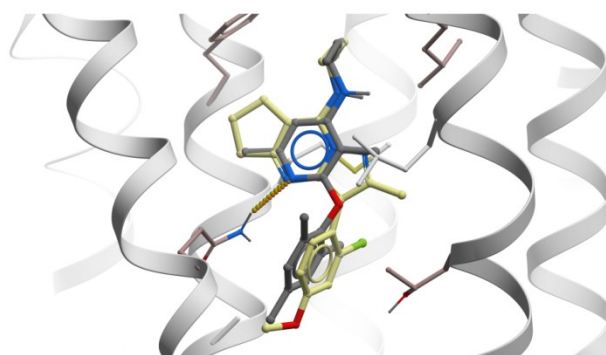


**Figure S9.** Docking of CP-376395 (grey carbons) and ONO-2333Ms (yellow carbons). Dotted lines display the H-bond to N283<sup>5.50</sup>. CRHR1 helices are displayed as light grey ribbons, and key interacting amino-acids as sticks. Color code: grey, carbon; blue, nitrogen; red, oxygen; green: chlorine.

## 2: On the synthetic strategy of ABP-09

A preliminary retrosynthetic analysis of the desired antagonist ABP-09, according to the synthetic schemes for asymmetric aza-dipyrromethenes more frequently used, <sup>[12]</sup> revealed the involvement of unstable intermediates and precursors. In this sense, the requirement of a 2,4-diaryl substitution pattern to obtain  $\alpha$ -nitroso pyrroles with acceptable yields has been discussed by others. <sup>[13, 14]</sup> In fact, the presence of at least one aryl substituent in position 2 of the pyrrole was considered to be essential to obtain an aza-BODIPY structure. <sup>[15]</sup>

Attempts in the literature to synthesize an aza-BODIPY from 3-ethyl-2,4-dimethyl-pyrrole

using the  $\text{NaNO}_2/\text{AcOH}$  route did not lead to the expected structure, but instead a 3-amine BODIPY isomer was obtained after an intramolecular redox reaction of the  $\alpha$ -nitroso pyrrole.<sup>[16]</sup> In the present work, we ruled out this possibility because the synthetic scheme selected avoided the *in situ* formation of the key  $\alpha$ -nitroso pyrrole, and  $\text{NaNO}_2$  was not used in any reaction step. On the other hand, it was demonstrated that the aza-BODIPY is formed after condensation between a pyrrole and a pyrrol-imine, or after pyrrol-imine auto-condensation.<sup>[17]</sup>

### 3: Solvatochromism of ABP-09

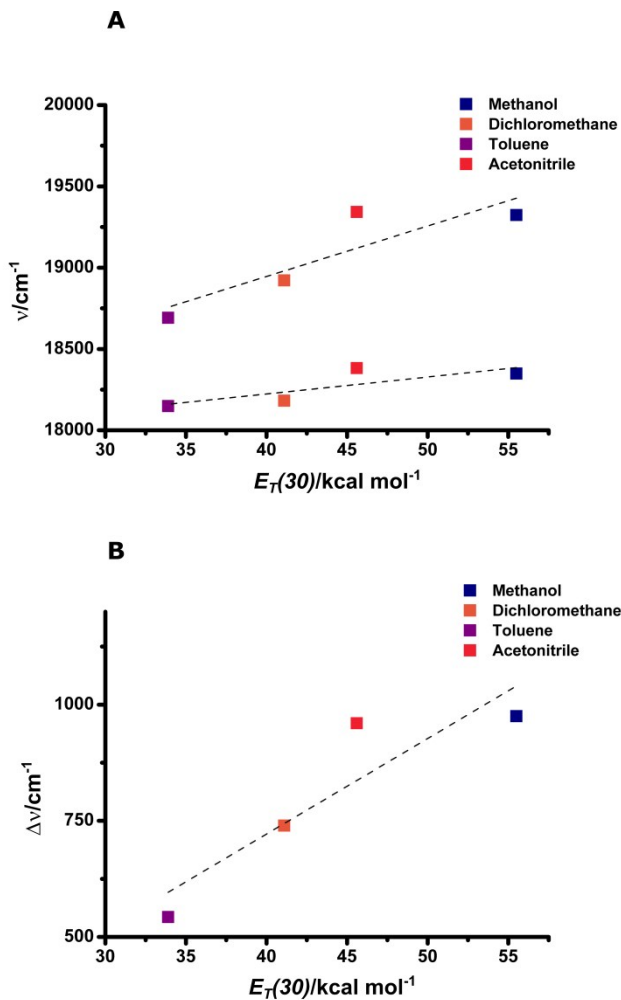


**Figure S10.** A) Energy of the maximum absorption (upper line and symbols) and emission (lower line and symbols) wavelength of ABP-09 as a function of the solvent parameter  $E_T(30)$ . B) Stokes shift of ABP-09 as a function of solvent parameter  $E_T(30)$ . For both plots solvents are: toluene (violet symbols), dichloromethane (orange symbols), acetonitrile (red symbols), and methanol (blue symbols).

#### 4: STORM performance of ABP-09 in cells

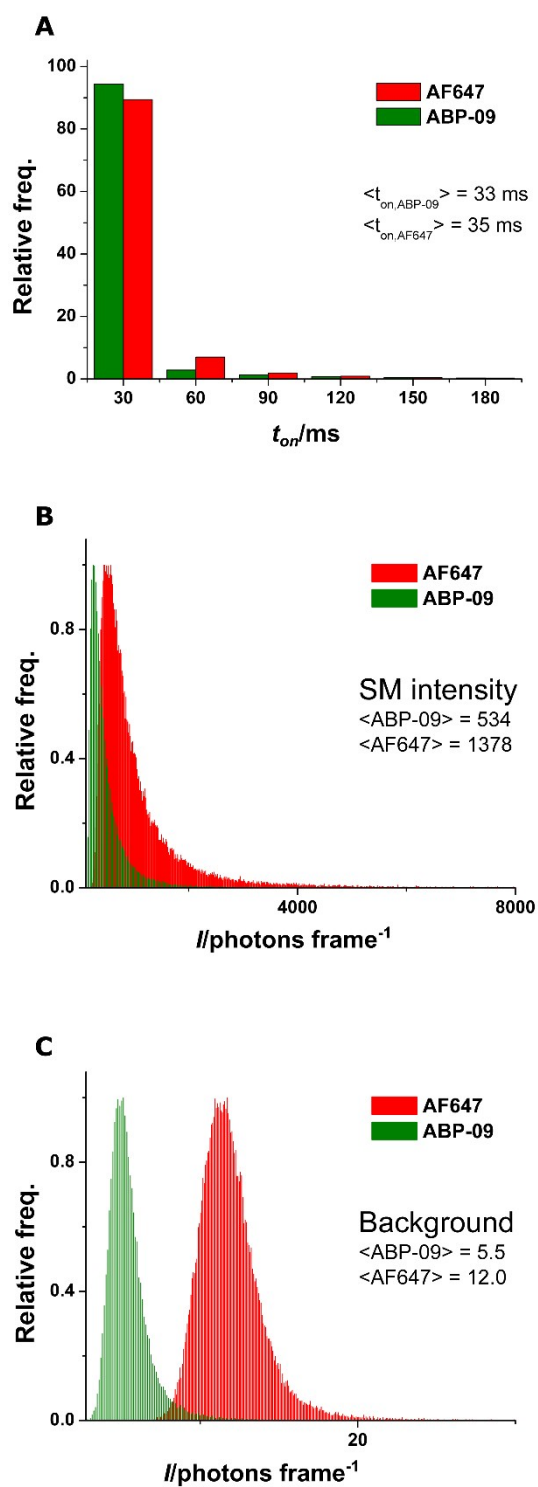


**Figure S11.** A) Histogram of ON times for ABP-09 and Alexa Fluor 647. An exposure time of 30 ms in both channels and an excitation laser power density of  $(6 \pm 1)\text{ kW}\cdot\text{cm}^{-2}$  in

each laser were used. B) Histogram of single molecules intensity in photon counts per frame for ABP-09 and Alexa Fluor 647 (same conditions as panel A). C) Histogram of background level for ABP-09 and Alexa Fluor 647 (same conditions as panel A).

### 5: Experiments in cells and estimation of the CRHR1-ABP-09 binding constant

Uptake of ABP-09 by HT22-CRHR1 cells was followed by live imaging (Figure S12). The time course of the brightness of ABP-09 emission after 100 nM or 10 nM addition of the dye in DMSO solution shows a fast incorporation, reaching a maximum in a few minutes after addition. Then, it is followed by a decay with a lifetime of ca 5 hours, attaining after 20 hours a plateau, which has the same brightness in the two concentrations tested. We took this experiment as a reference for the time of incubation with ABP-09 before experiments.

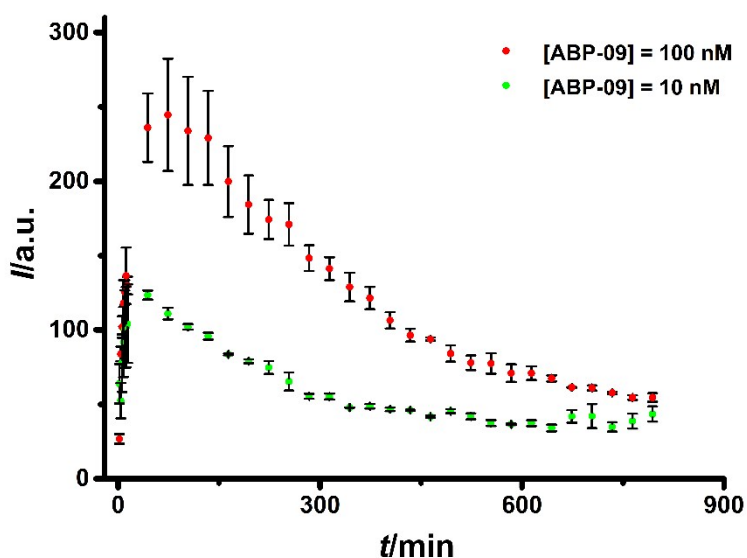


**Figure S12.** Incorporation of ABP-09 into HT22-CRHR1 cells. Time course of the fluorescence brightness monitored by live imaging fluorescence microscopy.

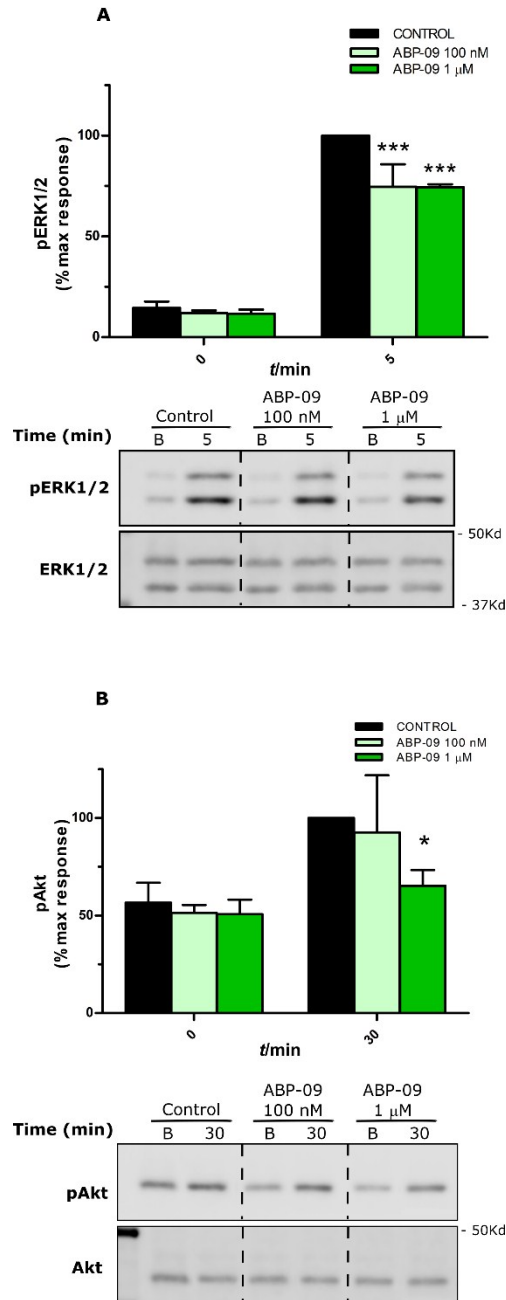


**Figure S13:** Effect of ABP-09 in the activation of ERK1/2 and Akt in HT22-CRHR1 cells. Effectors were measured in HT22-CRHR1 cells stimulated with 100 nM CRH for the indicated time, pERK1/2, pAkt, total ERK1/2, and total Akt were determined by Western Blot. Cells were preincubated for 20 h with indicated concentration of ABP-09 or vehicle (control). A) ERK1/2 activation. Results are expressed as the percentage of maximum pERK1/2 after stimulation under control conditions (mean  $\pm$  SEM n=3). \*\*\*,  $p < 0.001$  by two ways ANOVA followed by Bonferroni test. B) Akt activation. Results are expressed as the percentage of maximum pAkt after stimulation under control conditions (mean  $\pm$  SEM n=3). \*,  $p < 0.05$  by two ways ANOVA followed by Bonferroni test.

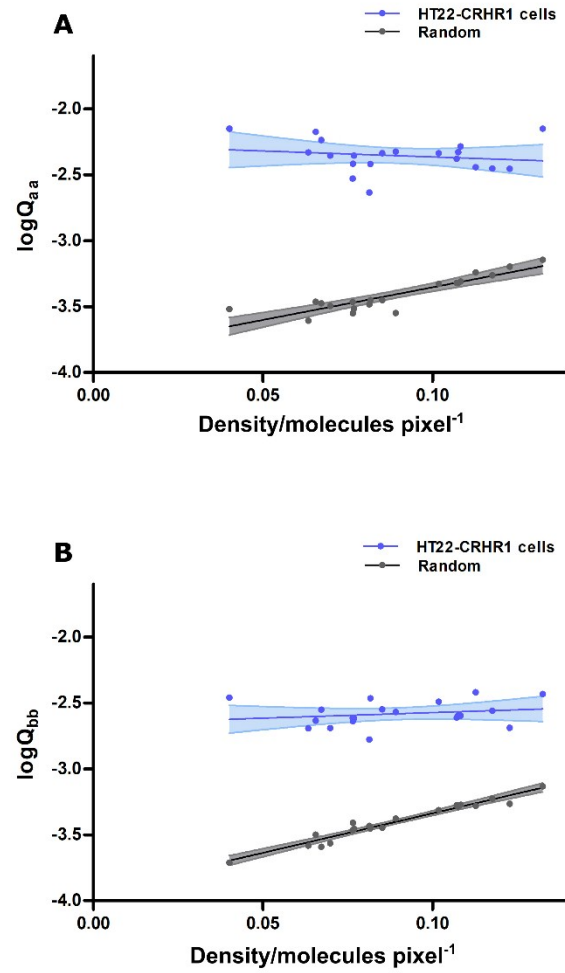


**Figure S14:** Plot of pairing coefficient  $Q_{ij}$  as a function of the average number of molecules per pixel in various portions of different cells for the actual (blue dots) and the simulated random distribution (black dots). “a” stands for Alexa Fluor 647 and “b” stands for ABP-09. A)  $Q_{aa}$  ; B)  $Q_{bb}$ .

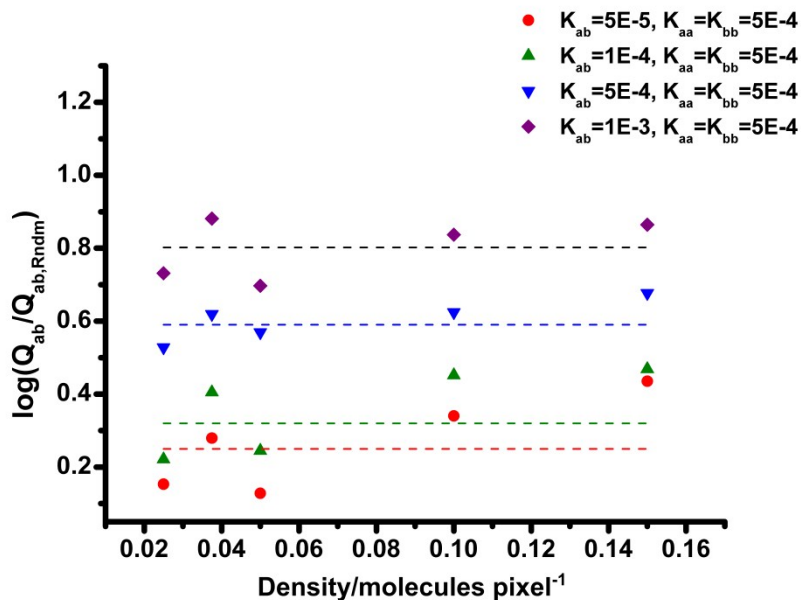


**Figure S15.** Logarithmic plot of  $Q_{ab}$  normalized to the value of the random distribution ( $Q_{ab,rdm}$ ) as a function of molecular density for different input values of the association equilibrium constants  $K_{ij}$ ,  $i, j = a, b$ . Data were obtained from simulations of molecular distributions.

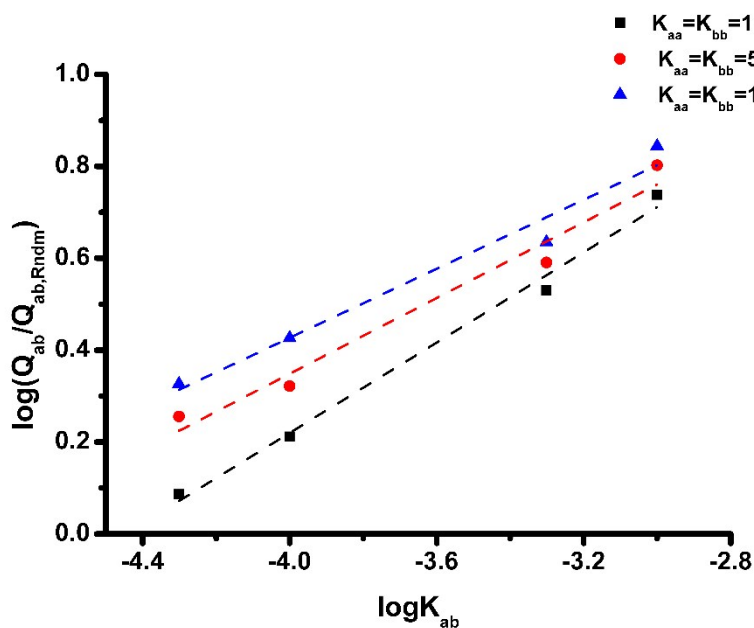


**Figure S16.** Plot of the average value of  $\log(Q_{ab}/Q_{ab,rdm})$  extracted from Figure S15, as a function of  $K_{ab}$ , for different values of  $K_{aa} = K_{bb}$ .

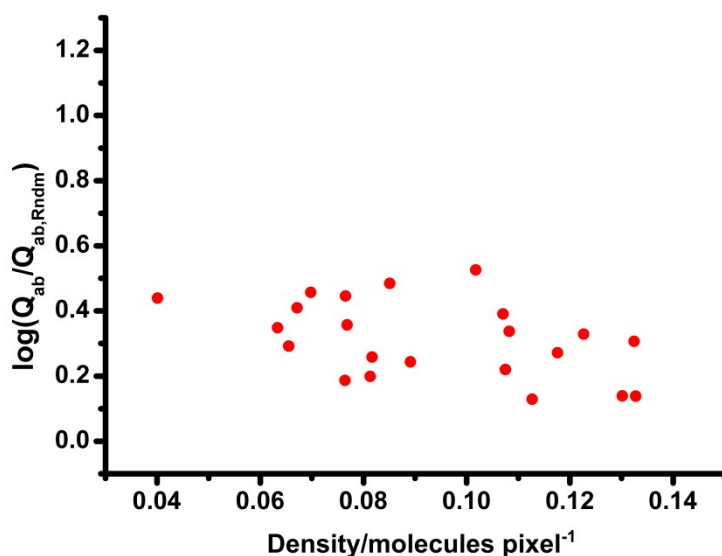


**Figure S17.** Plot of  $R_{ab} = \log(Q_{ab}/Q_{ab,rdm})$  as a function of molecular density for the experimental data of Figure 7A (main text). An average value with standard deviation of  $0.31 \pm 0.11$  is obtained for  $\log(Q_{ab}/Q_{ab,rdm})$ .

The value of  $R_{ab} = 0.31 \pm 0.11$  is used as input in calibration plot of Figure S16 to obtain the value for  $K_{ab}$ ,  $K_{aa}$ , and  $K_{bb}$  of the text, considering  $K_{aa} = K_{bb} > K_{ab}$ . These later considerations refer to blue and red curves of Figure S16.

**Movie S1.** Temporal evolution of emission arising from mTurquoise2, Venus and ABP-09 in HT22-CRHR1-EPAC-S<sup>H187</sup> cells (each emission channel is shown in a different column). At a certain time, cells were stimulated with CRH 10 nM ( $t=0$  in Figure 4). The conditions studied were: Control cells (untreated with antagonist) and cells pre-treated with either ABP-09 10 nM or ABP-09 100 nM (each condition is shown in a different row). An increase of mTurquoise2 emission is observed in Control cells after stimulating with CRH 10 nM, as well as a decrease of emission arising from Venus. This effect is due to a drop in FRET efficiency caused by cAMP increase. This change is less visible for cells treated with ABP-09, revealing a lower cAMP increment under those conditions. ABP-09 emission remains negligible and constant, even at the higher concentration used. The movie consists of 17 frames, shown at 5 fps, with a 15 seconds separation between frames. CRH addition occurs at frame 8, i.e., in the middle of the movie.

**Movie S2.** Fragment of STORM acquisition frame sequence in a single HT22-CRHR1 fixed cell, pretreated with ABP-09 10 nM and immunolabeled with Alexa Fluor 647. Both dyes were simultaneously excited and detected. Bright single molecule blinking can be observed in both channels. 41 frames are shown at 10 fps. Each frame corresponds to a time point of 30 ms.

## References

- [1] T. A. Halgren, *J. Am. Chem. Soc.* **1992**, *114*, 7827-7843.
- [2] T. A. Halgren, *J. Comp. Chem.* **1996**, *17*, 490-519.
- [3] T. A. Halgren, *J. Comp. Chem.* **1996**, *17*, 553-586.
- [4] T. A. Halgren, *J. Comp. Chem.* **1996**, *17*, 520-552.
- [5] T. A. Halgren, *J. Comp. Chem.* **1996**, *17*, 616-664.
- [6] Z. Wang, G. Yin, J. Qin, M. Gao, L. Cao, A. Wu, *Synthesis* **2008**, *22*, 3565-3568.
- [7] A. Gorman, J. Killoran, C. O'Shea, T. Kenna, W. M. Gallagher, D. F. O'Shea, *J. Am. Chem. Soc.* **2004**, *126*, 10619-10631.
- [8] D. Wu, D. F. O'Shea, *Org. Lett.* **2013**, *15*, 3392-3395.
- [9] J. J. Bonfiglio, C. Inda, S. Senin, G. Maccarrone, D. Refojo, D. Giacomini, C. W. Turck, F. Holsboer, E. Arzt, S. Silberstein, *Mol. Endocrinol.* **2013**, *27*, 491-510.
- [10] C. Inda, P. A. dos Santos Claro, J. J. Bonfiglio, S. A. Senin, G. Maccarrone, C. W. Turck, S. Silberstein, *J. Cell. Biol.* **2016**, *214*, 181-195.
- [11] F. M. Barabas, L. A. Masullo, F. D. Stefani, *Rev. Sci. Instr.* **2016**, *87*, 126103.
- [12] M. J. Hall, S. O. McDonnell, J. Killoran, D. F. O'Shea, *J. Org. Chem.* **2005**, *70*, 5571-5578.
- [13] Y. Ge, D. F. O'Shea, *Chem. Soc. Rev.* **2016**, *45*, 3846-3864.
- [14] Xin-Dong Jiang, D. Xi, J. Zhao, H. Yu, G.-T. Sunb, L.-J. Xiaoa, *RSC Advances* **4**, 60970-60973.
- [15] W. Zhao, E. Carreira, *Chem. Eur. J.* **2006**, *12*, 7254-7263.
- [16] M. Liras, J. B. Prieto, M. Pintado-Sierra, F. L. Arbeloa, I. García-Moreno, Á. Costela, L. Infantes, R. Sastre, F. Amat-Guerri, *Org. Lett.* **2007**, *9*, 4183-4186.
- [17] M. Grossi, A. Palma, S. O. McDonnell, M. J. Hall, D. K. Rai, J. Muldoon, D. F. O'Shea, *J. Org. Chem.* **2012**, *77*, 9304-9312.